The Journal of Clinical Endocrinology & Metabolism, 2022, **107**, e2291–e2300
https://doi.org/10.1210/clinem/dgac128
Advance access publication 05 March 2022
Clinical Research Article

The p300 Inhibitor A-485 Exerts Antitumor Activity in Growth Hormone Pituitary Adenoma

Chenxing Ji,[1,2,*] Wen Xu,[3,*] Hong Ding,[4,5,*] Zhengyuan Chen,[1,2,*] Chengzhang Shi,[1,2] Jie Han,[5] Liang Yu,[5] Nidan Qiao,[1,2,6] Yichao Zhang,[1,2,6] Xiaoyun Cao,[1,2,6] Xiang Zhou,[1,2,6] Haixia Cheng,[7] Huijin Feng,[8] Cheng Luo,[5] Zhiyu Li,[4], Bing Zhou,[8,9] Zhao Ye,[1,2,6], and Yao Zhao[1,2,6,10,11]

[1]Department of Neurosurgery, Huashan Hospital, Shanghai Medical College, Fudan University, National Center for Neurological Disorders, Shanghai 200040, China
[2]Neurosurgical Institute of Fudan University, Shanghai 200040, China
[3]Hospital & Institute of Obstetrics and Gynecology, Fudan University, Shanghai, 200011, China
[4]Department of Medicinal Chemistry, China Pharmaceutical University, Nanjing 211198, China
[5]Drug Discovery and Design Center, CAS Key Laboratory of Receptor Research, State Key Laboratory of Drug Research, Shanghai Institute of Materia Medica, Chinese Academy of Sciences, Shanghai 201203, China
[6]Shanghai Key laboratory of Brain Function Restoration and Neural Regeneration, Shanghai 200040, China
[7]Department of Pathology, Huashan Hospital, Shanghai Medical College, Fudan University, Shanghai 200040, China
[8]Department of Medicinal Chemistry, State Key Laboratory of Drug Research, Shanghai Institute of Materia Medica, Chinese Academy of Sciences, Shanghai 201203, China
[9]School of Pharmaceutical Science and Technology, Hangzhou Institute for Advanced Study, UCAS, Hangzhou 310024, China
[10]State Key Laboratory of Medical Neurobiology and MOE Frontiers Center for Brain Science, Institutes of Brain Science, Fudan University, Shanghai, China
[11]National Clinical Research Center for Aging and Medicine, Huashan Hospital, Fudan University, Shanghai 200040, China

Correspondence: Prof. Zhiyu Li, Department of Medicinal Chemistry, China Pharmaceutical University, 639 Long Mian Avenue, Jiangning, Nanjing, China. Email: zhiyuli@cpu.edu.cn; or Prof. Bing Zhou, Laboratory of Drug Research, Shanghai Institute of Materia Medica, Chinese Academy of Sciences, 555 Zu Chong Zhi Road, Zhang Jiang Hi-Tech Park, Pudong, Shanghai, China. Email: zhoubing@simm.ac.cn; or Doc. Zhao Ye, Department of Neurosurgery, Huashan Hospital, Shanghai Medical College, Fudan University, 958 Jin Guang Road, Minhang, Shanghai, China. Email: yezhaozj663812@126.com
*These authors contributed equally to this work.

Abstract

Context: Growth hormone pituitary adenoma (GHPA), a major subtype of pituitary adenoma (PA), can lead to progressive somatic disfigurement, multiple complications, and even increased mortality. The efficacy of current treatments is limited; thus, a novel pharmacological treatment is urgently needed. As a histone acetyltransferase (HAT) coactivator, p300 can regulate the transcription of several genes that are crucial for PA tumorigenesis and progression. However, the role of p300 and its catalytic inhibitor in GHPA is still unclear.

Objective: We aimed to identify the expression of p300 in GHPA and in normal pituitary glands.

Methods: The expression of p300 was detected in GHPA and normal pituitary tissues. Genetic knockdown was performed by siRNA. The efficacy of the p300 inhibitor A-485 in the cell cycle, proliferation, apoptosis, and hormone secretion was investigated by flow cytometry, ELISAs, Western blotting, and qRT-PCR. RNA sequencing, bioinformatic analysis, and subsequent validation experiments were performed to reveal the potential biological mechanism of A-485.

Results: High expression of p300 was found in GHPA tissues compared with normal pituitary tissues. Knockdown of *p300* inhibited cell proliferation and clone formation. Treatment with A-485 suppressed cell growth and inhibited the secretion of GH in vitro and in vivo. Further mechanistic studies showed that A-485 could downregulate the expression or activity of several oncogenes, such as genes in the *Pttg1, c-Myc*, cAMP and PI3K/AKT/mTOR signaling pathways, which are crucial for PA tumorigenesis and progression.

Conclusion: Our findings demonstrate that inhibition of HAT p300 by its selective inhibitor A-485 is a promising therapy for GHPA.

Key Words: p300, A-485, growth hormone pituitary adenoma

Abbreviations: cAMP, cyclic adenosine monophosphate; ELISA, enzyme-linked immunosorbent assay; GH, growth hormone; GHPA, growth hormone pituitary adenoma; GO, Gene Ontology; H3K18, histone H3 lysine 18; H3K27, histone H3 lysine 27; HAT, histone acetyltransferase; IGF-1, insulin-like growth factor 1; IHC, immunohistochemistry; KEGG, Kyoto Encyclopedia of Genes and Genomes; PA, pituitary adenoma; qRT-PCR, quantitative reverse-transcriptase polymerase chain reaction; siRNA, small interfering RNA; SSA, somatostatin analogues.

Pituitary adenomas (PAs) are one of the most common intracranial neoplasms, with a prevalence of 10% to 25% (1-3). Based on immunohistochemical staining of the hormone content and primary transcription factors in the tumor, PAs can be classified into several subtypes. Overall, growth hormone pituitary adenomas (GHPAs) constitute approximately 20% of all PAs (4-6). Although the majority of GHPAs are benign, prolonged exposure to excess hormone can lead to

Received: 4 October 2021. **Editorial Decision:** 1 March 2022. **Corrected and Typeset:** 29 March 2022

progressive somatic disfigurement and a wide range of systemic manifestations, such as gigantism in children and acromegaly in adults. Terminally, the patients will present with cardiovascular, metabolic, respiratory, neoplastic, endocrine, articular, and bone complications, which are associated with increased mortality (7-10).

Treatment strategies for GHPA aim to control tumor growth and normalize growth hormone (GH) levels, thereby ameliorating the symptoms and reducing mortality (11, 12). As the cornerstone treatment, transsphenoidal adenomectomy is effective in approximately 75% of microadenomas (8). However, remission is not achieved in 50% of invasive macroadenomas (13-16). Pharmacological treatment also has an important role in the management of GHPA. Generally, treatment consists of somatostatin analogs (SSA), growth hormone receptor antagonist (GHR antagonists), and dopamine receptor agonists (DA). Nevertheless, all 3 of these medications have limited efficacy, with remission rates of 10% to 35% (17-22). Radiation is indicated as a third-line therapy after unsuccessful surgery and medical therapy, and biochemical control is only achieved in 50% of GHPA patients (23, 24). Thus, it is urgently necessary and practicably feasible to discover new therapeutic targets and medications for GHPA.

The pathogenesis of GHPA is complex and remains elusive. Current studies indicate that abnormal expression of functional genes, disruption of the cell cycle and dysregulation of signal transduction are associated with the tumorigenesis of GHPA. Emerging evidence has also shown that histone acetylation contributes to the pathogenesis of GHPA (25-27). As a key member of the histone acetyltransferase (HAT) family, p300 can modulate the transcriptional process by acetylating the histone tail or through protein-protein interactions with transcription factor (28). Aberrant expression of p300 has been involved in various cancers and is closely correlated with poor prognosis and a malignant phenotype (29-32). Several studies have shown that p300 can regulate the expression of pituitary tumor transforming gene 1 (*PTTG1*) and *c-MYC* and facilitate the transcriptional activity of *cAMP* (33-35). All 3 of these genes are essential for tumorigenesis and GH secretion (36-38). Moreover, a potent, selective, and drug-like catalytic p300 inhibitor, A-485, has been discovered and shown to have a more pronounced antitumor effect than previous inhibitors (39). It can specifically inhibit p300 catalyzed acetylation of histone H3 lysine 27 (H3K27) and lysine 18 (H3K18) sites (39, 40). However, the role of p300 and its inhibitor in GHPA remains unclear.

Therefore, the aim of the present study was to identify the expression of p300 in GHPA and in normal pituitary glands. Then, the role of p300 in the GHPA phenotype was assessed by genetic knockdown experiments and treatment with the pharmacological inhibitor A-485 in vivo and in vitro. Our findings suggest that inhibition of p300 with its selective inhibitor A-485 could serve as a potential therapeutic strategy for the treatment of GHPA in the future.

Methods

Patients and Tissue Samples

GHPA tissues were surgically removed at the Neurosurgery Department, Huashan Hospital, Fudan University. Histological diagnoses were performed independently by 2 experienced pathologists, according to the 2017 World Health Organization classification. Three normal pituitary tissues were obtained from cadaveric organ donations with no evidence of any endocrine disease (Fudan University). For immunohistochemistry (IHC) study, a total of 39 GHPA samples were collected. For Western blotting and qRT-PCR, 5 GHPA samples were included. The clinical characteristics are shown in Supplementary Table 1 (41).

Cell Culture

The rat pituitary adenoma GH3 cells (Cat. No. CCL-82.1), MMQ cells (Cat. No. CRL-10609), and mouse pituitary adenoma AtT-20 cells (Cat. No. CCL-89) were purchased from the ATCC and cultured in Ham's F-12K medium (Shanghai Basalmedia Technologies Co., Ltd.) with 15% horse serum (Gibco), 2.5% fetal bovine serum (FBS, Gibco) and 1% penicillin/streptomycin (Gibco). All the cells were maintained in an incubator at 37 °C supplemented with 5% CO_2.

Immunohistochemistry

Paraffin sections of GHPA and normal pituitary tissues were dewaxed by xylene and dehydrated by gradient ethanol. Incubation was at room temperature with 3% H_2O_2 for 5 to 10 minutes and then sections were washed in distilled water. The sections were blocked with 5% goat serum at room temperature for 10 minutes and incubated with primary antibody at 4 °C overnight. The next day, HRP-labeled secondary antibody incubation was carried out at room temperature for 30 minutes after washing in PBS. Then, DAB reagent was used to stain in proper time. Finally, the nuclei were re-stained with Harris hematoxylin (blue), washed, dehydrated in gradient ethanol and xylene, and then mounted with permanent mounting medium. The immune-reactivity was measured and quantified with Image-Pro Plus 6.0.

Western Blotting Analysis

Protein isolation was performed as previously described (42), ground tissues and cell lysates were separated on SDS-polyacrylamide gels and transferred to nitrocellulose membranes (Millipore). Membranes were blocked with a Tris/saline solution containing 5% skim milk and 0.1% Tween-20 at room temperature for 1 hour, and incubated with a primary antibody overnight at 4 °C. The next day, membranes were washed with TBST buffer, and then incubated with HRP–conjugated secondary antibody with a 1:10 000 dilution at room temperature for 1 hour. After 3 washings with TBST buffer, the bands were detected in a ChemiScope 3400 imaging system using ECL substrate (Cat. No. 32106, Thermo Scientific). The catalog number of antibodies are listed in Supplementary Table 2 (41). All experiments were repeated 3 times.

RNA Extraction and Quantitative Reverse-Transcriptase Polymerase Chain Reaction

Trizol reagent (Cat. No. R401-01, Vazyme Biotech) was used to isolate total RNA according to the manufacturer's protocol. Reverse transcription was carried out to obtain cDNA using HiScript II qRT SuperMix (Cat. No. R222-01, Vazyme Biotech). Subsequently, quantitative reverse-transcriptase polymerase chain reaction (qRT-PCR) was performed using AceQ qPCR SYBR Green Master Mix (Cat. No. Q141-02, Vazyme Biotech), and amplification was detected with a Quant Studio 6 Flex Real-Time PCR System

(ABI). Expression of target genes was normalized with the expression of GAPDH. The fold changes in gene expression were calculated using the equation $\Delta\Delta Ct = \Delta Ct$ (GENE-GAPDH)$_{normal}$ – ΔCt (GENE-GAPDH)$_{cancer}$. The primer sequences are listed in Supplementary Table 3 (41).

RNA Interference

Before transfection, a density of 1×10^6 GH3 cells/well were seeded into a 6-well plate. Transfection of small interfering RNA (siRNA) was performed with RNAiMAX reagent (Cat. No. 13778075, Invitrogen). After 48 hours of transfection, cells were collected for further experiments. The siRNA of p300 and negative control were synthesized by Shanghai Genepharma Co., Lid.

Cell Viability Assay

For the siRNA-treated GH3 cells, a density of 5×10^3 cells/well were seeded into a 96-well plate after 24 hours transfection. Cell viability assessments were performed at 24, 48, 72, and 96 hours. The A-485 treated GH3 cells were seeded at a density of 5×10^3 cells into 96-well plates incubated with dimethyl sulfoxide (DMSO; control) or a series of 2-fold-diluted concentrations of A-485 for 4 days. After that, Cell Titer-Glo luminescent assays (Cat. No. G7572, Promega) were performed to measure cell viability following the manufacturer's protocol, and the luminescence was monitored with a multifunctional microplate reader (EnVision, Perkin Elmer). Finally, the IC_{50} values were calculated in GraphPad Prism 7.0.

Clone Formation Assay

For the siRNA-treated GH3 cells, 1×10^3 transfected or control cells/well of each group were seeded in a 6-well plate. For the A-485 treated cells, 2×10^3 cells/well were seeded in a 6-well plate and incubated with A-485 or DMSO after 24 hours of adhesion. The cell medium containing A-485 was changed every 3 days. After 3 weeks of growth, all the colonies were fixed with 4% paraformaldehyde and then stained with 0.1% crystal violet. The clone formation assay was counted with Image-Pro Plus 6.0.

Cell Cycle and Apoptosis Assay

GH3 cells were seeded at a concentration of 1×10^6 cells/well in a 6-well plate and incubated with different concentration of A-485 for 72 hours. For the cell cycle assay, cells were collected and re-suspended in 70% ethanol overnight at 4 °C. Then, the samples were washed with PBS and stained with propidium iodide (PI, Cat. No. A211-01, Vazyme Biotech) for 30 minutes at room temperature. For the apoptosis assay, cells were incubated with a FITC-labeled annexin V and propidium iodide for 10 minutes. BD FACSCalibur (BD Pharmingen) was applied to analyze the cell cycle phase distribution and apoptosis according to the manufacturer's protocol (https://www.bdbiosciences.com/content/dam/bdb/marketing-documents/BD_FACSCalibur_instructions.pdf).

Enzyme-Linked Immunosorbent Assay

The supernatant of GH3 cells treated with A-485 after 24 hours and the blood of xenograft mice through eyeball method in serum were used to detect the concentrations of growth hormone by enzyme-linked immunosorbent assay using the Rat/Mouse GH ELISA kit (Cat. No. EZRMGH-45K, RRID: AB_2892711, https://antibodyregistry.org/search.php?q=AB_2892711, Merck Millipore). All of the ELISA experiments were carried out strictly following the kit protocol (https://www.sigmaaldrich.cn/CN/zh/product/mm/ezrmgh?context=produc).

Xenograft Experiment

Male BALB/c nude mice (6 to 8 weeks old) were selected for the GH3 xenograft model. A density of 2.5×10^6 GH3 cells suspension mixed with Matrigel Matrix (Cat. No. 354262, Corning) were injected into subcutaneous tissue of each mouse. When the tumor formed, all the mice were randomly divided into 3 groups with 8 mice in each group (A-485 100 mg/kg, A-485 50 mg/kg, and DMSO control). Tumor volumes was measured every 2 days and calculated as width^2 × length × 0.5. A-485 was intraperitoneally injected once daily when the tumor volumes approached about 100 mm^3. All the mice were sacrificed after a 28-day experiment, and the tumors were excised, weighed, and frozen at –80 °C. The blood specimens were collected from the orbit and frozen at –80 °C.

RNA Sequencing Analysis

A concentration of 1×10^7 GH3 cells were seeded in 10-cm dish plates and incubated with 5 μM A-485, 2.5 μM A-485, or DMSO for 48 hours. After that, cells were harvested and total RNA was isolated for preparation of cDNA library and then sequenced on Illumina Novaseq platform. Differential gene expression analysis was performed using the DESeq2 R package (1.16.1). The resulting *P* values were adjusted using Benjamini and Hochberg's approach for controlling the false discovery rate. Corrected *P* value of 0.05 and absolute foldchange of 2 were set as the threshold for significantly differential gene expression. Kyoto Encyclopedia of Genes and Genomes (KEGG) database (http://www.genome.jp/kegg/) and Gene Ontology (GO) enrichment analysis were used for further analysis for gene-annotation enrichment.

Statistical Analysis

All numerical results were expressed as the mean ± SD and represented data from a minimum of 3 independent experiments. A two-tailed unpaired *t* test was used to analyze differences between 2 groups. All analyses were performed using GraphPad Prism 7.0 statistical software (GraphPad Software, Inc., La Jolla, CA, USA). The level of statistical significance was set at $P < 0.05$.

Study Approval

This study was approved by the Ethics and Research Committees of Huashan Hospital, Fudan University. Tumor samples and corresponding clinical materials were obtained with the written consent from all patients. All the animal experiments were performed according to the ethical guidelines and approved by the Institute Animal Care and Use Committee (IACUC), Shanghai Institute of Materia Medica (SIMM), Chinese Academy of Sciences.

Results

p300 Expression Profile in GHPA and Normal Pituitary Gland

To assess the expression of p300 in GHPA tissues compared with that in normal pituitary tissues, we detected the protein and mRNA levels of p300 by IHC, Western

blotting, and qRT-PCR. This clearly showed an increase in p300 expression in GHPA tissues compared to normal pituitary tissues (Fig. 1A-1D), and p300 expression was relatively higher in the GH3 cell line (secreting GH and prolactin) than in the MMQ cell line (secreting prolactin), AtT-20 cell line (secreting ACTH) and normal rat pituitary tissue as a control (Supplementary Figure 1 (41)). Hence, we selected the GH3 cell line for subsequent experiments. Analyzing the correlation between the expression of p300 and the clinical data, we found that the expression of p300 was positively correlated with the preoperative GH level and insulin-like growth factor-1 (IGF-1) index (upper limit of normal range for age- and sex-matched IGF-1 level) (Supplementary Figure 2a and 2b (41)). As the patients with suppression rate of octreotide suppression test (OST) above 90.51% (43) are considered as SSA sensitive, we divided them into SSA responders and SSA nonresponders. Here, the expression of p300 in the SSA nonresponders exhibited an increasing trend compared to that in the SSA responders. It indicated that p300 might be involved in SSA resistance, although there was no significant difference ($P = 0.08$) (Supplementary Figure 2c (41)). Overall, the high expression of p300 and its positive correlation with adverse clinical features established the theoretical foundation for subsequent studies.

Knockdown of p300 Suppresses Cell Proliferation in GH3 Cells

To elucidate the functional role of p300 in GHPA, p300-specific siRNAs were constructed and transfected into GH3 cells. The knockdown efficiency was validated by Western blotting and qRT-PCR (Fig. 2A and 2B). As the most effective siRNA, siRNA-p300#3 remarkably inhibited the levels of the specific acetylation targets H3K18ac and H3K27ac (Fig. 2C); thus, it was chosen for further experiments. Notably, knockdown of p300 significantly inhibited GH3 cell proliferation ($P < 0.001$) and reduced clone formation ($P < 0.001$) (Fig. 2D and 2E). Taken together, our

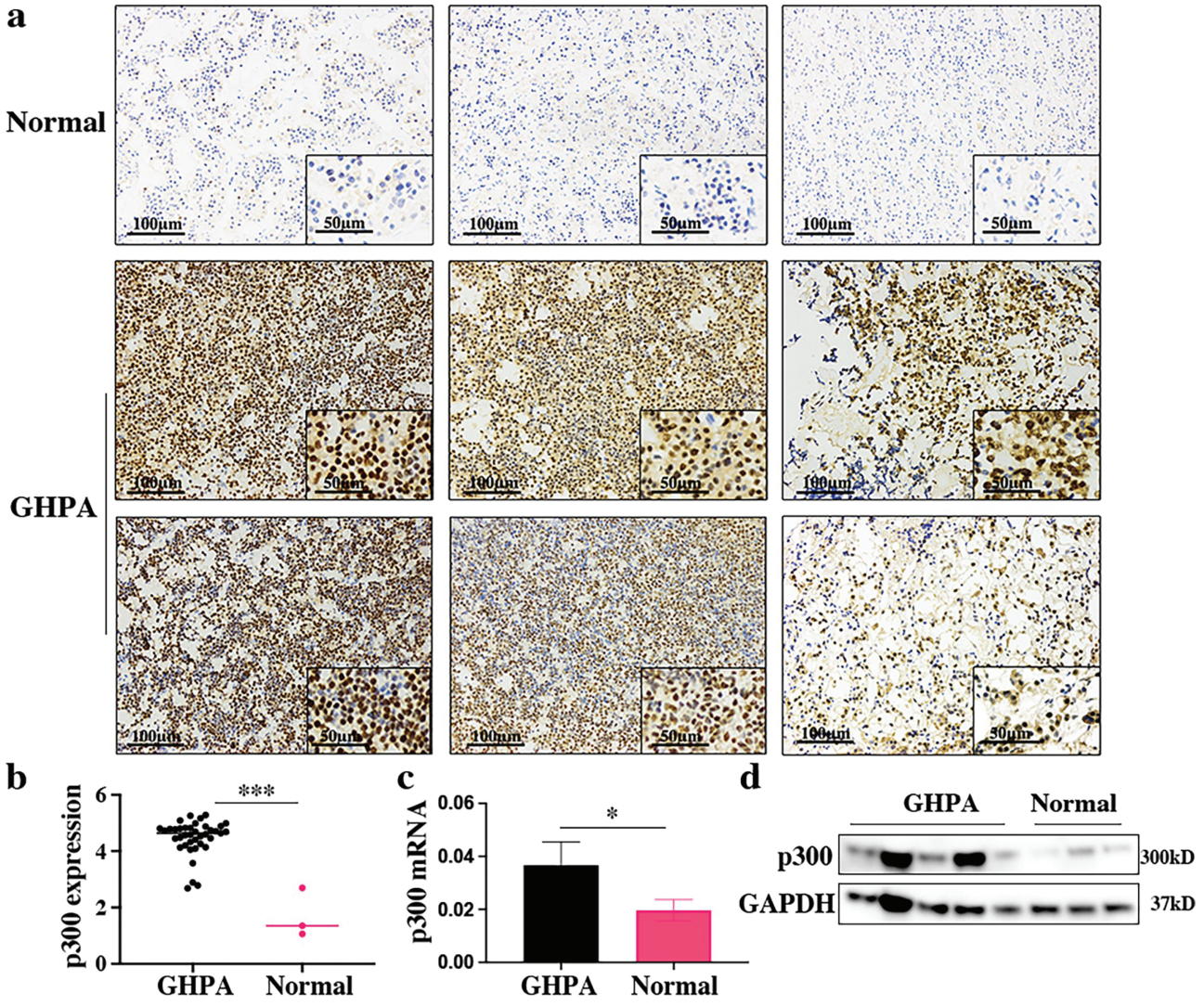

Figure 1. p300 expression profile in GHPA and normal pituitary tissue. (a) IHC image of p300 expression in normal pituitary and GHPA tissues. Each column represents a different sample. Scale bars: 100 μm left, 50 μm right. (b) Logarithmized IOD value of p300 expression according to IHC images of GHPA tissues (n = 39) and normal pituitary tissues (n = 3). (c) The mRNA expression of p300 in specimens (GHPA: n = 5; Normal: n = 3) assessed by qRT-PCR. (d) The protein expression of p300 in specimens (GHPA: n = 5; Normal: n = 3) assessed by Western blotting. $*P < 0.05$, $**P < 0.01$, $***P < 0.001$. The bar represents ± SD.

data suggest that p300 exerts a crucial effect on the proliferation of GH3 cells.

p300 Inhibitor A-485 Reduces Cell Viability and GH Secretion In Vitro

To investigate the potential therapeutic effect of the p300 catalytic inhibitor A-485 on GH3 cells, CellTiter Glo was performed to evaluate cell viability. The IC_{50} was 0.489 μM after 3 days of A-485 treatment (Fig. 3A). A-485 significantly induced the dose-dependent and time-dependent inhibition of cell proliferation in GH3 cells (Fig. 3B). Gratifyingly, the levels of H3K18ac and H3K27ac were also decreased after treatment with A-485, suggesting that the antiproliferative effect of A-485 was associated with enzymatic inhibition of its target p300 in GHPA cells (Fig. 3C). After 72 hours of incubation with A-485 at concentrations of 5 μM, 2.5 μM, 1.25 μM, and 0 μM, flow cytometry was carried out to detect the cell cycle and apoptosis. Clearly, A-485 treatment increased the percentage of apoptotic cells (Fig. 3D) and the protein expression of the apoptosis marker cleaved caspase 3 (Supplementary Figure 3a (41)). In addition, A-485 induced G2/M phase arrest in GH3 cells (Fig. 3E) and inhibited the expression of the G2/M phase-related protein cyclin B1 (Supplementary Figure 3b (41)). To evaluate the long-term inhibitory effect of A-485 on GH3 cells, a clone formation assay was performed. Prolonged exposure to A-485 at concentrations of 0.5 μM ($P < 0.0001$) and 1 μM ($P < 0.0001$) for 3 weeks significantly inhibited the colonization of GH3 cells (Fig. 3F). Furthermore, we tested the mRNA expression of *Gh1* and evaluated the secretion of growth hormone after treatment of cells with A-485. It was clear that A-485 inhibited *Gh1* mRNA expression and secretion ability in GH3 cells (Fig. 3G and 3H). In summary, these data suggest that A-485, a highly selective catalytic inhibitor of p300, can inhibit the development of malignant phenotypes and reduce GH expression in GH3 cells.

p300 Inhibitor A-485 Reduced Tumor Survival and GH Secretion In Vivo

To evaluate the antitumor effects of the p300 selective inhibitor A-485 in vivo, we generated a subcutaneous xenograft model with GH3 cells in BALB/c nude mice. Treatment with A-485 significantly inhibited tumor growth with regard to tumor volume (32.37% inhibition in the 50 mg/kg group and 54.15% inhibition in the 100 mg/kg group) and tumor weight (43.83% inhibition in the 50 mg/kg group and 61.41% inhibition in the 100 mg/kg group) in comparison with the control regimen (Fig. 4A and 4B, Supplementary Figure 4 (41)). Mouse body weight was increased in the control group, due to hypersecretion of GH, and A-485 clearly reduced the weight in the treatment group (Fig. 4C). Additionally, ELISA was performed to explore GH secretion in serum. As expected, serum GH secretion was significantly reduced in the A-485-treated mice (Fig. 4D).

p300 Inhibitor A-485 Effects on Gene Expression in GH3 Cells

To explore the antitumor molecular mechanism of A-485 in GHPA, RNA sequencing analysis was applied. The differentially expressed genes were revealed in heatmaps and volcano plot maps. Among them, 2750 upregulated genes and 2625 downregulated genes or 435 upregulated genes and 392 downregulated genes were observed in cells treated with 5 μM or 2.5 μM A-485, respectively (Fig. 5A, Supplementary Figure 5 (41)). Venn diagrams show the overlapping genes for treatments with different concentrations. There were 732 genes that showed differential expression at both concentrations (Fig. 5B). The fold changes in hub genes are shown in Fig. 5C, which were verified by qRT-PCR (Fig. 5D). Among the hub genes,

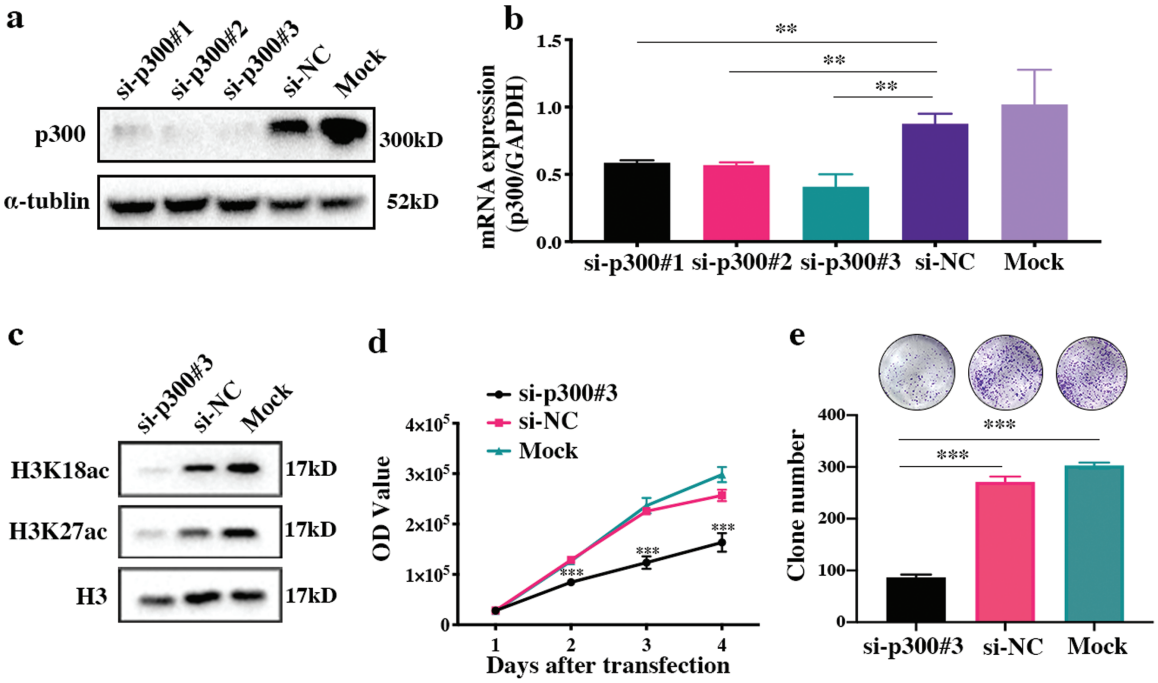

Figure 2. Knockdown of p300 inhibits cell proliferation, clone formation, and the acetylation of H3. (a, b) The protein and mRNA expression of p300 in GH3 cells after transfection with p300-siRNAs, the negative control, and the mock control. (c) The protein expression of H3K18ac and H3K27ac in p300-knockdown GH3 cells. (d) Cell proliferation of p300-knockdown GH3 cells. (e) Clone formation by p300-knockdown GH3 cells. $*P < 0.05$, $**P < 0.01$, $***P < 0.001$. The bar represents ± SD.

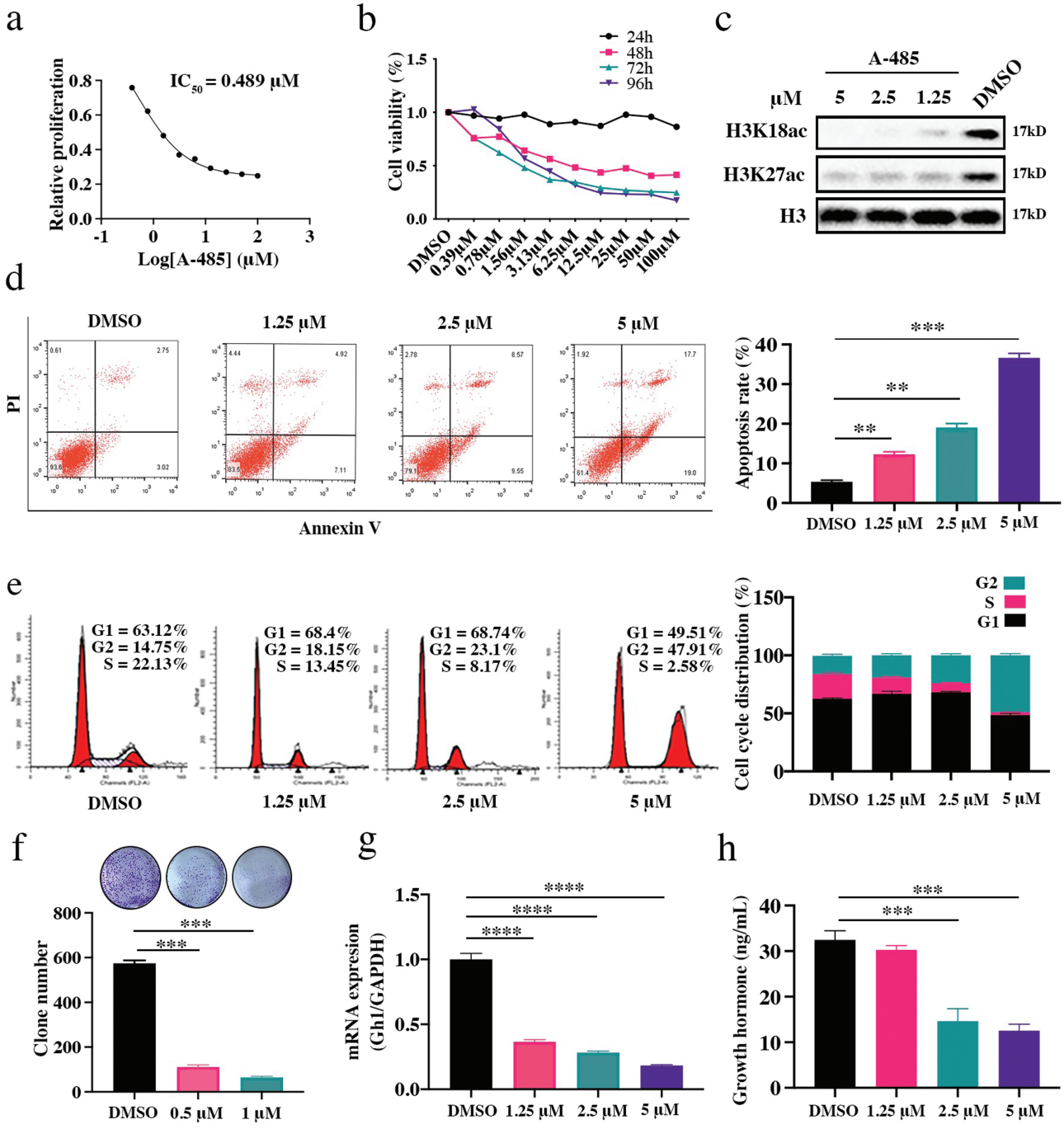

Figure 3. The p300 inhibitor A-485 exerts antitumor effects in vitro. (a) The IC_{50} of A-485 in GH3 cells was detected after 3 days of A-485 incubation. (b) The cell viability was detected at 24, 48, 72, and 96 hours, respectively. (c) The protein expression of H3K18ac and H3K27ac in A-485 treated GH3 cells. (d) Apoptosis analysis of A-485 treated GH3 cells. (e) Cell cycle analysis of A-485 treated GH3 cells. (f) Clone formation of A-485 treated GH3 cells. (g) The mRNA expression of *Gh1* in A-485 treated GH3 cells. (h) The secretion of GH in the supernatant of A-485 treated GH3 cells. $^{*}P < 0.05$, $^{**}P < 0.01$, $^{***}P < 0.001$, $^{****}P < 0.0001$. The bar represents ± SD.

Pttg1 and *Gh1* were downregulated, which has previously been reported to be related to the occurrence and development of GHPA. Also, *Cdk1 and Ccnb1* were downregulated and are known to be cell cycle–related genes. GO enrichment analysis of biological processes and molecular functions showed that most hub genes functioned in chromosome segregation and cell cycle processes (Supplementary Figure 6 (41)). KEGG analysis indicated that the PI3K/Akt/mTOR signaling pathway was specifically affected by A-485 (Fig. 5E). As crucial molecules in the PI3K/Akt/mTOR pathway, the phosphorylation of Akt, mTOR, and S6K was verified by Western blotting. A-485 inhibited the phosphorylation level of these proteins (Fig. 5F). Moreover, A-485 reduced the expression of c-Myc and inhibited the phosphorylation of Creb, which are crucial in GHPA oncogenicity and essential in GH secretion (Fig. 5F).

Discussion

GHPA usually possesses 2 main pathophysiological characteristics, the occupying effect and hypersecretion of GH,

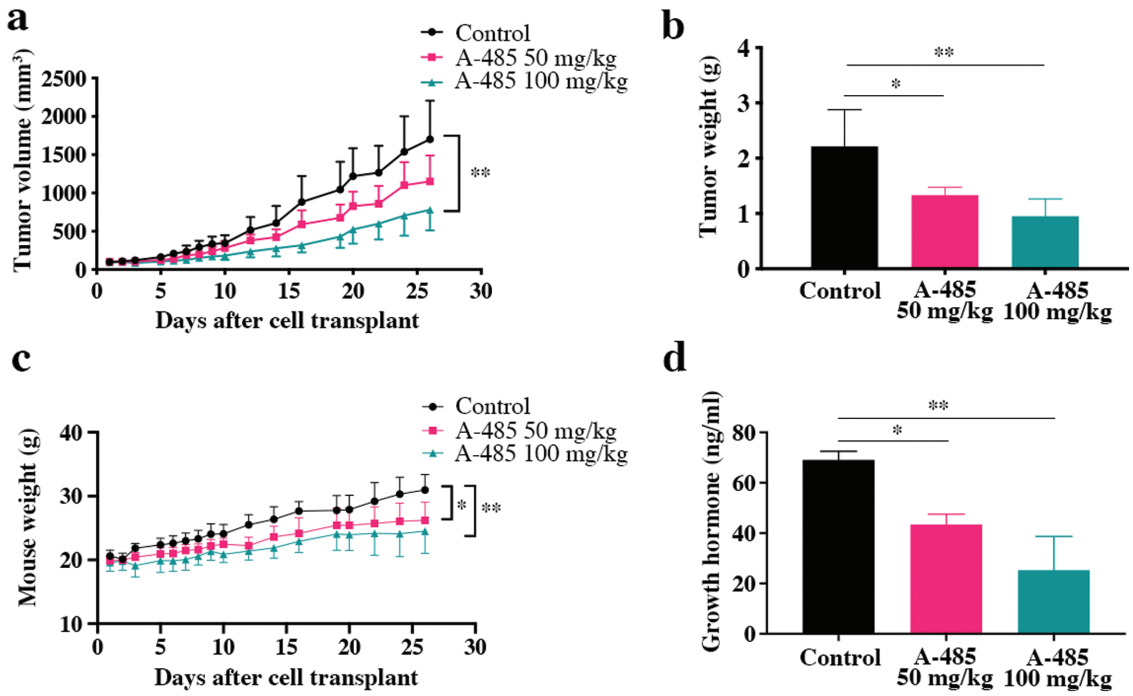

Figure 4. The antitumor effect of A-485 in vivo. (a, b, c) The tumor volume, tumor weight, and mouse weight of each group during the experiment are shown. (d) The level of growth hormone in serum was detected by ELISA assays. *$P < 0.05$, **$P < 0.01$, ***$P < 0.001$. The bar represents ± SD.

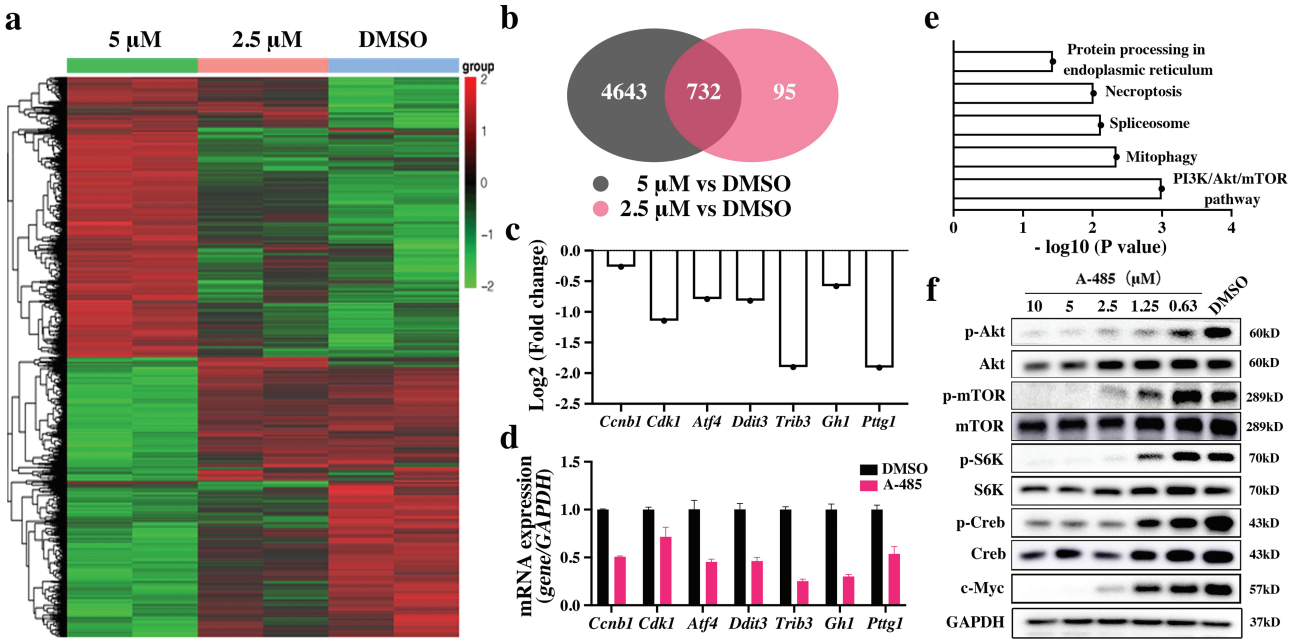

Figure 5. Exploration of the potential mechanism affected by A-485. (a) Heat maps of differentially expressed genes at different concentrations of A-485. (b) Venn diagrams showing the overlapping genes between each group. (c) The fold changes in hub genes based on the RNA sequencing. (d) The mRNA expression of hub genes was verified by qRT-PCR. (e) KEGG analysis indicated the specific signaling pathways affected by A-485. (f) The protein expressions of key molecules affected by A-485 were detected by Western blotting. The bar represents ± SD.

which result in severe clinical symptoms and multisystemic comorbidities that shorten the lifespan of patients by 10 to 20 years (7-10). Hence, therapeutic strategies for GHPA aim to control tumor growth and to achieve biochemical remission, and these strategies remain challenging. As mentioned above, transsphenoidal surgery can achieve satisfactory remission rates in microadenoma and intrasellar macroadenoma. However, the effect is much lower in invasive macroadenoma with suprasellar or/and parasellar expansion, and the recurrence rate is high due to active cell proliferation (13-16). For medical therapy, drug resistance is still a large obstacle. Therefore, novel therapeutic targets and drugs are urgently needed.

Currently, increasing attention has been given to the function of epigenetic alterations, particularly abnormal levels of histone acetylation in the progression of PA, which would

provide novel insights into PA treatment (25-27). The levels of acetylation in the histone tail, especially H3 and H4, could be considered active markers that are regulated by HATs and histone deacetylases (HDACs). As a crucial member of the HAT family, p300 can regulate gene expression and facilitate transcriptional activity. p300 is overexpressed in various cancers, such as liver tumors (31), nasopharyngeal tumors (32) and hemopathy (44). There is also a strong correlation between high expression of p300 and poor prognosis in these tumors, indicating that p300 promotes tumor growth. More intriguingly, in prostate cancer, p300 is not only involved in the progression of cancer cells but also impacts the secretion of androgen (30). Since GHPA is a hormone-secreting tumor, we were intensely curious about the role of p300 in GHPA. Overexpression of *PTTG1* and *c-MYC* has been shown to be positively correlated with tumor invasiveness, aggressiveness, or recurrence in GHPA (36, 37, 45, 46), and p300 can regulate the expression of these 2 crucial genes (33, 34). In addition, p300 can facilitate transcription factor binding to the promoter region during the transcription of cyclic adenosine monophosphate (cAMP), and activation is of cAMP is highly associated with GH secretion and somatotroph proliferation (38, 47). Thus, we assumed that p300 plays a critical role in the development of GHPA and sought to validate our hypothesis through a series of experiments.

In our study, we demonstrated that the expression of p300 was elevated in GHPA tissues compared with normal pituitary tissues. Subsequent analysis of clinical data showed that the expression of p300 was positively correlated with the preoperative GH level and the IGF-1 index, which was in line with the key characteristic of GHPA. In addition, the expression of p300 in the SSA responders group exhibited a higher trend than that in the control group, indicating that p300 might be involved in SSA resistance. There was no significant difference ($P = 0.08$), but this was probably due to the insufficient number of GHPA patients who received medical therapy before surgery. Consistent with the results observed in other cancers described above, the increased expression of p300 in GHPA and its correlation with clinical features provide the theoretical basis for targeting p300 for GHPA treatment.

Consequently, functional assays involving both genetic knockdown of *p300* and treatment with A-485, a highly selective catalytic inhibitor, could lead to significant inhibition of cell proliferation and clone formation of GH3 cells in vitro. Flow cytometry assays and the expression of related markers indicated that the growth inhibition of GH3 cells is due to the induction of apoptosis and G2/M cell cycle arrest by A-485. Strikingly, A-485 significantly inhibited the mRNA expression and secretion of GH in vitro. Subsequently, the pharmacological efficacy of A-485 was evaluated in a subcutaneous xenotransplantation model. In agreement with the efficacy observed in vitro, A-485 effectively inhibited tumor growth and GH secretion. These therapeutic effects of A-485 in vitro and in vivo suggest that p300 inhibitors might serve as potential candidates for GHPA therapy.

To explore the mechanism by which A-485 inhibits GHPA tumorigenesis, transcriptome sequencing analysis was performed. The results of the GO enrichment analysis showed that the most highly differentially expressed genes were enriched in chromosome segregation, the cell cycle, and other biological processes. Another bioinformatic analysis of KEGG enrichment revealed that the main pathways influenced by A-485 include the cell cycle pathway and the PI3K/Akt/mTOR pathway. The PI3K/Akt/mTOR pathway is involved in numerous cellular processes, such as cell growth, the cell cycle, and protein synthesis. Its aberrant activation has been confirmed to be associated with the malignant behavior of cancers including glioma, breast cancer, and ovarian cancer. Based on previous studies, aberrant activation of the PI3K/Akt/mTOR pathway has been confirmed to contribute to malignant proliferation (48-51) and hormone secretion in GHPA (52, 53). Through the application of the mTOR inhibitor rapamycin or RAD001, clear inhibition of the viability and proliferation of GHPA cells was induced (53, 54). Similarly, the dual-PI3K/mTOR inhibitor XL765 inhibited GHPA cell growth but showed drug toxicity and produced no significant differences in GH secretion in vivo (55). Compared with the inhibitors described above, A-485 shows great advantages (a lower IC_{50} and effective inhibition of GH secretion in vivo) in terms of antitumor effects. However, the expression of phosphorylated Akt, S6K, and mTOR was also decreased, suggesting that the antitumor effects of A-485 may occur through inhibition of the PI3K/Akt/mTOR pathway. Moreover, A-485 led to the downregulation of *c-Myc*, *Pttg1*, and *Gh1*, which participate in tumorigenesis and function in GHPA. Furthermore, the expression of phosphorylated Creb was also downregulated by A-485. It has been demonstrated that Creb acts as a crucial transcriptional regulator in the cAMP signaling pathway, which is closely related to GH secretion (38, 47).

In summary, our findings highlight the significance of p300 in the tumorigenesis of GHPA, suggesting that p300 may serve as a novel therapeutic target. The antitumor effect of the p300 inhibitor A-485 in vitro and in vivo demonstrates that A-485 might serve as a potential therapeutic for GHPA.

Acknowledgments

We gratefully acknowledge Mrs. Yun Zhang, Mrs. Ye Wang, Mrs. Qiuyue Wu, and Mrs. Lan Lai for sample collection. We thank Mrs. Jingjing Zhu, Mr. Chao Li, and Mrs. Liyan Yue for technical support.

Funding

This study was supported by the Ministry of Science and Technology of China (National Key R&D Program of China, 2017YFB0202600), the "Personalized Medicines Molecular Signature-based Drug Discovery and Development" (Strategic Priority Research Program of the Chinese Academy of Sciences, XDA12020368) to Hong Ding; the National Natural Science Foundation of China (81802496), the Shanghai Sailing Program (18YF1402700) to Zhao Ye; the China Pituitary Adenoma Specialist Council (CPASC), the National High Technology Research and Development Program of China (863 program, 2014AA020611), the Chang Jiang Scholars Program, the National Program for Support of Top-Notch Young Professionals, the National Science Fund for Distinguished Young Scholars (81725011) to Yao Zhao;

Author Contributions

Conception or design of the work: Zhao Ye, Yao Zhao, and Bing Zhou. Financial support: Hong Ding, Zhao Ye, and Yao

Zhao. Subject recruitment: Yao Zhao, Xiaoyun Cao, Xiang Zhou, Zhao Ye, and Yichao Zhang. Pathological diagnosis: Haixia Cheng. Inhibitor synthesis: Huijin Feng and Bing Zhou. Laboratory Practice: Chenxing Ji, Hong Ding, and Zhengyuan Chen. Xenograft Experiment: Jie Han, Liang Yu, and Chengzhang Shi. Data analysis and interpretation: Chenxing Ji, Hong Ding, Zhengyuan Chen, and Zhao Ye. Drafting the article: Chenxing Ji, Wen Xu, and Nidan Qiao. Critical revision of the article: Zhiyu Li, Yao Zhao, and Cheng Luo. All authors critically reviewed the article and approved the final manuscript.

Disclosures

The authors declare no potential conflicts of interest.

Data Availability

All data generated or analyzed during this study are included in this published article.

References

1. Ostrom QT, Gittleman H, Liao P, *et al*. CBTRUS statistical report: primary brain and central nervous system tumors diagnosed in the United States in 2007-2011. *Neuro Oncol*. 2014;16(Suppl 4):iv1-iv63.
2. Agustsson TT, Baldvinsdottir T, Jonasson JG, *et al*. The epidemiology of pituitary adenomas in Iceland, 1955-2012: a nationwide population-based study. *Eur J Endocrinol*. 2015;173(5):655-664.
3. Dal J, Feldt-Rasmussen U, Andersen M, *et al*. Acromegaly incidence, prevalence, complications and long-term prognosis: a nationwide cohort study. *Eur J Endocrinol*. 2016;175(3):181-190.
4. Hoskuldsdottir GT, Fjalldal SB, Sigurjonsdottir HA. The incidence and prevalence of acromegaly, a nationwide study from 1955 through 2013. *Pituitary*. 2015;18(6):803-807.
5. Arosio M, Reimondo G, Malchiodi E, *et al*. Predictors of morbidity and mortality in acromegaly: an Italian survey. *Eur J Endocrinol*. 2012;167(2):189-198.
6. Molitch ME. Diagnosis and treatment of pituitary adenomas: a review. *JAMA*. 2017;317(5):516-524.
7. Theodros DP, Ruzevick J, Lim M, Bettegowda C. Pituitary adenomas: historical perspective, surgical management and future direction. review. *CNS Oncology*. 2015;4(6):411-429.
8. Colao A, Grasso LFS, Giustina A, *et al*. Acromegaly. *Nat Rev Dis Primers*. 2019;5(1):20.
9. Sherlock M, Ayuk J, Tomlinson JW, *et al*. Mortality in patients with pituitary disease. *Endocr Rev*. 2010;31(3):301-342.
10. Ritvonen E, Loyttyniemi E, Jaatinen P, *et al*. Mortality in acromegaly: a 20-year follow-up study. *Endocr Relat Cancer*. 2016;23(6):469-480.
11. Katznelson L, Laws ER Jr, Melmed S, *et al*. Acromegaly: an Endocrine Society clinical practice guideline. *J Clin Endocrinol Metab*. 2014;99(11):3933-3951.
12. Melmed S, Bronstein MD, Chanson P, *et al*. A consensus statement on acromegaly therapeutic outcomes. *Nat Rev Endocrinol*. 2018;14(9):552-561.
13. Chen CJ, Ironside N, Pomeraniec IJ, *et al*. Microsurgical versus endoscopic transsphenoidal resection for acromegaly: a systematic review of outcomes and complications. *Acta Neurochir (Wien)*. 2017;159(11):2193-2207.
14. Starke RM, Raper DM, Payne SC, Vance ML, Oldfield EH, Jane JA Jr. Endoscopic vs microsurgical transsphenoidal surgery for acromegaly: outcomes in a concurrent series of patients using modern criteria for remission. *J Clin Endocrinol Metab*. 2013;98(8):3190-3198.
15. Kim JH, Hur KY, Lee JH, *et al*. Outcome of Endoscopic Transsphenoidal Surgery for Acromegaly. *World Neurosurg*. 2017;104:272-278.
16. Babu H, Ortega A, Nuno M, *et al*. Long-Term Endocrine Outcomes Following Endoscopic Endonasal Transsphenoidal Surgery for Acromegaly and Associated Prognostic Factors. *Neurosurgery*. 2017;81(2):357-366.
17. Howlett TA, Willis D, Walker G, Wass JA, Trainer PJ; UK Acromegaly Register Study Group (UKAR-3). Control of growth hormone and IGF1 in patients with acromegaly in the UK: responses to medical treatment with somatostatin analogues and dopamine agonists. *Clin Endocrinol (Oxf)*. 2013;79(5):689-699.
18. Melmed S, Cook D, Schopohl J, Goth MI, Lam KS, Marek J. Rapid and sustained reduction of serum growth hormone and insulin-like growth factor-1 in patients with acromegaly receiving lanreotide Autogel therapy: a randomized, placebo-controlled, multicenter study with a 52 week open extension. *Pituitary*. 2010;13(1):18-28.
19. Sesmilo G, Resmini E, Bernabeu I, *et al*. Escape and lipodystrophy in acromegaly during pegvisomant therapy, a retrospective multicentre Spanish study. *Clinical Endocrinology*. 2014;81(6):883-890.
20. Neggers SJ, Franck SE, de Rooij FW, *et al*. Long-term efficacy and safety of pegvisomant in combination with long-acting somatostatin analogs in acromegaly. *J Clin Endocrinol Metab*. 2014;99(10):3644-3652.
21. Ben-Shlomo A, Liu NA, Melmed S. Somatostatin and dopamine receptor regulation of pituitary somatotroph adenomas. *Pituitary*. 2017;20(1):93-99.
22. Colao A, Auriemma RS, Pivonello R, Kasuki L, Gadelha MR. Interpreting biochemical control response rates with first-generation somatostatin analogues in acromegaly. *Pituitary*. 2016;19(3):235-247.
23. Abu Dabrh AM, Asi N, Farah WH, *et al*. Radiotherapy Versus Radiosurgery in Treating Patients with Acromegaly: A Systematic Review and Meta-Analysis. *Endocr Pract*. 2015;21(8):943-956.
24. Gheorghiu ML. Updates in outcomes of stereotactic radiation therapy in acromegaly. *Pituitary*. 2017;20(1):154-168.
25. Ebrahimi A, Schittenhelm J, Honegger J, Schluesener HJ. Histone acetylation patterns of typical and atypical pituitary adenomas indicate epigenetic shift of these tumours. *J Neuroendocrinol*. 2011;23(6):525-530.
26. Bilodeau S, Vallette-Kasic S, Gauthier Y, *et al*. Role of Brg1 and HDAC2 in GR trans-repression of the pituitary POMC gene and misexpression in Cushing disease. *Genes Dev*. 2006;20(20):2871-2886.
27. Wang W, Fu L, Li S, Xu Z, Li X. Histone deacetylase 11 suppresses p53 expression in pituitary tumor cells. *Cell Biol Int*. 2017;41(12):1290-1295.
28. Bedford DC, Kasper LH, Fukuyama T, Brindle PK. Target gene context influences the transcriptional requirement for the KAT3 family of CBP and p300 histone acetyltransferases. *Epigenetics*. 2010;5(1):9-15.
29. Iyer NG, Ozdag H, Caldas C. p300/CBP and cancer. *Oncogene*. 2004;23(24):4225-4231.
30. Debes JD, Sebo TJ, Lohse CM, Murphy LM, Haugen DA, Tindall DJ. p300 in prostate cancer proliferation and progression. *Cancer Res*. 2003;63(22):7638-7640.
31. Li M, Luo RZ, Chen JW, *et al*. High expression of transcriptional coactivator p300 correlates with aggressive features and poor prognosis of hepatocellular carcinoma. *J Transl Med*. 2011;9:5. doi:10.1186/1479-5876-9-5
32. Liao ZW, Zhou TC, Tan XJ, *et al*. High expression of p300 is linked to aggressive features and poor prognosis of nasopharyngeal carcinoma. *J Transl Med*. 2012;10:110. doi:10.1186/1479-5876-10-110
33. Li T, Huang H, Huang B, Huang B, Lu J. Histone acetyltransferase p300 regulates the expression of human pituitary tumor transforming gene (hPTTG). *J Genet Genomics*. 2009;36(6):335-342.
34. Ogiwara H, Sasaki M, Oike T, Higuchi S, Tominaga Y, Kohno T. Targeting p300 addiction in CBP-deficient cancers causes synthetic

lethality by apoptotic cell death due to abrogation of MYC expression. *Cancer Discov*. 2016;6(4):430-445.
35. Gomez RA, Pentz ES, Jin X, Cordaillat M, Sequeira Lopez ML. CBP and p300 are essential for renin cell identity and morphological integrity of the kidney. *Am J Physiol Heart Circ Physiol*. 2009;296(5):H1255-H1262.
36. Pei L, Melmed S. Isolation and characterization of a pituitary tumor-transforming gene (PTTG). *Mol Endocrinol*. 1997;11(4):433-441.
37. Liu C, Wu Y, Yu S, *et al*. Increased betacatenin and c-myc expression predict aggressive growth of non-functioning pituitary adenomas: An assessment using a tissue microarray-based approach. *Mol Med Rep*. 2017;15(4):1793-1799.
38. Ben-Shlomo A, Deng N, Ding E, *et al*. DNA damage and growth hormone hypersecretion in pituitary somatotroph adenomas. *J Clin Invest*. 2020;130(11):5738-5755.
39. Lasko LM, Jakob CG, Edalji RP, *et al*. Discovery of a selective catalytic p300/CBP inhibitor that targets lineage-specific tumours. *Nature*. 2017;550(7674):128-132.
40. Weinert BT, Narita T, Satpathy S, *et al*. Time-Resolved Analysis Reveals Rapid Dynamics and Broad Scope of the CBP/p300 Acetylome. *Cell*. 2018;174(1):231-244.e12.
41. Chenxing J. A-485 GHPA supplementary materials. *figshare*. Figure. Posted January 31, 2022. https://doi.org/10.6084/m9.figshare.19096541.v1
42. Chen Z, Zhang H, Liu S, *et al*. Discovery of novel trimethoxy-ring BRD4 bromodomain inhibitors: AlphaScreen assay, crystallography and cell-based assay. *Medchemcomm*. 2017;8(6):1322-1331.
43. Wang M, Shen M, He W, *et al*. The value of an acute octreotide suppression test in predicting short-term efficacy of somatostatin analogues in acromegaly. *Endocr J*. 2016;63(9):819-834.
44. Giotopoulos G, Chan WI, Horton SJ, *et al*. The epigenetic regulators CBP and p300 facilitate leukemogenesis and represent therapeutic targets in acute myeloid leukemia. *Oncogene*. 2016;35(3):279-289.
45. Xiao JQ, Liu XH, Hou B, *et al*. Correlations of pituitary tumor transforming gene expression with human pituitary adenomas: a meta-analysis. *PLoS One*. 2014;9(3):e90396.
46. Woloschak M, Roberts JL, Post K. c-myc, c-fos, and c-myb gene expression in human pituitary adenomas. *J Clin Endocrinol Metab*. 1994;79(1):253-257.
47. Hernandez-Ramirez LC, Trivellin G, Stratakis CA. Cyclic 3',5'-adenosine monophosphate (cAMP) signaling in the anterior pituitary gland in health and disease. *Mol Cell Endocrinol*. 2018;463:72-86.
48. Monsalves E, Juraschka K, Tateno T, *et al*. The PI3K/AKT/mTOR pathway in the pathophysiology and treatment of pituitary adenomas. *Endocr Relat Cancer*. 2014;21(4):R331-R344.
49. Sajjad EA, Zielinski G, Maksymowicz M, Hutnik L, Bednarczuk T, Wlodarski P. mTOR is frequently active in GH-secreting pituitary adenomas without influencing their morphopathological features. *Endocr Pathol*. 2013;24(1):11-19.
50. Musat M, Korbonits M, Kola B, *et al*. Enhanced protein kinase B/Akt signalling in pituitary tumours. *Endocr Relat Cancer*. 2005;12(2):423-433.
51. Sajjad EA, Zielinski G, Maksymowicz M, Hutnik L, Bednarczuk T, Wlodarski P. mTOR is frequently active in GH-secreting pituitary adenomas without influencing their morphopathological features. *Endocr Pathol*. 2013;24(1):11-19.
52. Di Pasquale C, Gentilin E, Falletta S, *et al*. PI3K/Akt/mTOR pathway involvement in regulating growth hormone secretion in a rat pituitary adenoma cell line. *Endocrine*. 2018;60(2):308-316.
53. Xie R, He WQ, Shen M, *et al*. Specific inhibition of mTOR pathway induces anti-proliferative effect and decreases the hormone secretion in cultured pituitary adenoma cells. *J Neurooncol*. 2015;125(1):79-89.
54. Gorshtein A, Rubinfeld H, Kendler E, *et al*. Mammalian target of rapamycin inhibitors rapamycin and RAD001 (everolimus) induce anti-proliferative effects in GH-secreting pituitary tumor cells in vitro. *Endocr Relat Cancer*. 2009;16(3):1017-1027.
55. Dai C, Zhang B, Liu X, *et al*. Inhibition of PI3K/AKT/mTOR pathway enhances temozolomide-induced cytotoxicity in pituitary adenoma cell lines in vitro and xenografted pituitary adenoma in female nude mice. *Endocrinology*. 2013;154(3):1247-1259.